FUDMA Journal of Sciences (FJS)
ISSN online: 2616-1370
ISSN print: 2645 - 2944
Vol. 5 No. 1, March, 2021, pp 16 – 26
DOI: https://doi.org/10.33003/fjs-2021-0501-508

CASSON FLUID OF A STAGNATION-POINT FLOW (SPF) TOWARDS A VERTICAL SHRINKING/STRETCHING SHEET

[1]Winifred N. Mutuku, *[2]Anselm O. Oyem

[1]Department of Mathematics and Actuarial Science, Kenyatta University, Nairobi, Kenya
*[2]Department of Mathematical Sciences, Federal University Lokoja, Kogi State, Nigeria

*Corresponding Author's Email: anselmoyemfulokoja@gmail.com

ABSTRACT

This study presents a convectively heated hydromagnetic Stagnation-Point Flow (SPF) of an electrically conducting Casson fluid towards a vertically stretching/shrinking sheet. The Casson fluid model is used to characterize the non-Newtonian fluid behaviour and using similarity variables, the governing partial differential equations are transformed into coupled nonlinear ordinary differential equations. The dimensionless nonlinear equations are solved numerically by Runge-Kutta Fehlberg integration scheme with shooting technique. The effects of the thermophysical parameters on velocity and temperature profiles are presented graphically and discussed quantitatively. The result shows that the flow field velocity decreases with increase in magnetic field parameter and Casson fluid parameter β.

Keywords: Biot number; Fluid flow; Stream function; RK-Fehlberg integration scheme; Lorentz force.

INTRODUCTION

An electrically conducting hydromagnetic viscous incompressible boundary layer flow fluid with a convective surface boundary condition is frequently used in many areas of biological, industrial and technological applications (Mutuku, 2014). Some of these applications includes extrusion of plastics in the manufacture of rayon and nylon, MHD (magnetohydrodynamic) blood flow meters and generators, cooling of nuclear reactors, geothermal energy extraction, and drag reduction in aerodynamics, purification of crude oil, textile, polymer technology, and metallurgy, among others. Since inception on MHD boundary layer flows research (Sakiadis, 1961), various authors have investigated numerous aspects of steady and unsteady boundary layer flow of a convective fluids as well as nanofluids (Makinde and Aziz, 2010; Bachok *et al*., 2012; Mutuku and Makinde, 2014; Khan and Khan, 2016; Makinde, 2012).

Stagnation-point fluid (SPF) flow over a continuously stretching/shrinking surface is significantly relevant in many engineering and industrial processes such as extraction of polymer sheet, polymer processing, paper production, glass blowing, glass-fibre production, plastic films drawing, filaments drawn through a quiescent electrically conducting fluid and the purification of molten metals from non-metallic inclusions. The stretching surface and heat transfer is controlled for superior products since the final product quality depends on the rate of cooling and many aspects of this problem have been investigated by several other authors (Chen *et al*., 1970; Gupta and Gupta, 1977; Chiam, 1994; Layek *et al*., 2007; Makinde and Aziz, 2011; Crane, 2018).

Non-Newtonian fluid flows are expressed in several engineering processes (oil reservoir engineering, bioengineering), geophysics, chemical and nuclear industries, polymer solution, cosmetic processes, paper production, design of thrust bearings and radial diffusers among others. These fluids exhibit a nonlinear relationship between shear stress and rate of strain which deviate significantly from the Newtonian fluid (Navier-Stokes) model making it difficult to express these properties in a single constitutive equation. Owing to the complexity of these fluids, there is not a single constitutive equation which exhibits all their properties thus, amongst the different types of non-Newtonian fluids namely; viscoelastic fluid, couple stress fluid, micropolar fluid, power-law flow and Casson fluid, various models have been used for non-Newtonian fluids, with their constitutive equations varying greatly in complexity (Fox *et al*., 1969; Lun-Shin and Manun, 2008; Xu and Shi-Jun, 2009; Reddy *et al*., 2012).

Casson fluids behave like an elastic solid, with a yield shear stress existing in the constitutive equation. It is a shear thinning liquid assumed to have an infinite viscosity at zero rate of shear, a yield stress below which no flow occurs, and a zero viscosity at an infinite rate of shear. This implies that if a shear stress greater than yield stress is applied, it starts to move whereas if a shear stress less than the yield stress is applied to the fluid, it behaves like a solid. Examples include yoghurt, molten chocolate, cosmetics, nail polish, tomato puree, jelly, honey, soup, concentrated fruit juices, human blood, amongst others. Casson (1959) investigated the flow behaviour of pigment oil suspensions of the printing ink type. Medikare *et al*., (2016) looked at MHD stagnation-point flow of a Casson fluid over a nonlinearly stretching sheet with viscous dissipation.

Due to novelty, several studies on Casson fluid pertaining to different flow situations have taken center stage on contemporary research in fluid sciences and engineering which includes; Musatafa *et al*., 2011; Bhattacharyya and Vajravelu, 2012; Shehzad *et al*. 2013; Nandy, 2013; Bhattacharyya *et al*., 2013; Bhattacharyya, 2013a; Bhattacharyya, 2013b; Mukhopadhyay *et al*., 2013; Mutuku and Makinde, 2013; Pramanik, 2014; Mutuku, 2014; Shateyi and Marewo, 2014; Hussain *et al*., 2015; Saidulu and Lakshmi, 2016; Medikare *et al*., 2016; Mutuku, 2016; Ouru, *et al*., 2016; Medikare *et al*., 2016; Mabood *et al*., 2017; Seth *et al*., 2017; Mutuku and Makinde, 2017; El-Aziz and Yahya, 2017; Sheikh and Abbas, 2017; Singh *et al*., 2018; Gangadhar *et al*., 2018 and Sobamowo *et al*., 2019.

Despite the numerous applications of non-Newtonian fluids in industrial and engineering processes, deficiency from the above literatures in hydromagnetic Casson fluid flow has raised a strong motivation towards understanding its behaviour in several transport processes hence, this study. This study therefore extends the work of Medikare *et al*., (2016) by incorporating buoyancy force and considering a convective boundary layer in the numerical analysis of the hydromagnetic stagnation-point flow of a steady, incompressible Casson fluid towards a shrinking/stretching sheet.

MATHEMATICAL FORMULATION

Consider a steady, incompressible two-dimensional SPF (Stagnation-Point Fluid) flow of an electrically conducting Casson fluid towards a vertically stretching/shrinking sheet at $y = 0$ with the flow confined in the region $y > 0$. Along the stretching surface in the x-axis, two equal and opposite forces are being applied with a uniform magnetic field strength B_0 applied perpendicular to the surface. The induced magnetic field is neglected while the ambient fluid is moved with a velocity $U_\infty(x) = ax$. The equation of state for an isotropic and incompressible flow of a Casson fluid (Bhattacharyya, 2013a; 2013b) is given by

$$\tau_{ij} = \left(\mu_B + \frac{P_y}{\sqrt{2\pi}}\right)2e_{ij}\,,\ \ \pi > \pi_c\ \left(\mu_B + \frac{P_y}{\sqrt{2\pi_c}}\right)2e_{ij}\,,\ \ \pi > \pi_c \tag{1}$$

where π is the product of the component of deformation rate with itself, $\pi = e_{ij}e_{ij}$; e_{ij} are the $(i,j)^{th}$ components of the deformation rate and π_c is a critical value of this product based on the non-Newtonian model, μ_B is plastic dynamic velocity of the non-Newtonian fluid and P_y is the yield stress of the fluid.

The MHD boundary layer equations for the steady incompressible SPF is given by

$$\frac{\partial u}{\partial x} + \frac{\partial v}{\partial y} = 0 \tag{2}$$

$$u\frac{\partial u}{\partial x} + v\frac{\partial u}{\partial y} = U_\infty\frac{dU_\infty}{dx} + v\left(1+\frac{1}{\beta}\right)\frac{\partial^2 u}{\partial y^2} + \beta g(T - T_\infty) - \frac{\sigma B_0^2 x}{\rho}(u - U_\infty) \tag{3}$$

$$u\frac{\partial T}{\partial x} + v\frac{\partial T}{\partial y} = \alpha\frac{\partial T}{\partial y} + \frac{\alpha\mu}{k}\left(1+\frac{1}{\beta}\right)\left(\frac{\partial u}{\partial y}\right)^2 + \frac{\sigma\alpha B_0^2 x}{k}(u - U_\infty)^2. \tag{4}$$

The boundary conditions at the sheet surface and free stream are:

$$u(x,0) = U_w(x)\ \ ,\ \ v(x,0) = 0,\ \ -k_f\frac{\partial T}{\partial y}(x,0) = h_f\left(T_f - T(x,0)\right)\quad at \quad y = 0, \tag{5}$$

$$u(x,0) \to U_\infty(x),\ \ T(x,\infty) \to T_\infty \qquad as \qquad y \to \infty. \tag{6}$$

Where u, v are the velocity components in x, y directions respectively, ρ is the viscosity, $\beta = \mu_B\sqrt{\frac{2\pi_c}{P_y}}$ is the non-Newtonian or Casson parameter, $U_w = bx$ is the shrinking/stretching velocity for the sheet with b being the shrinking/stretching constant, $b < 0$ corresponds to shrinking, $b > 0$ corresponds to stretching and $U_\infty = ax$ is straining velocity of the stagnation point flow with $a(> 0)$ being straining constant.

The stream functions $u = \partial\psi/\partial y$ and $v = -\partial\psi/\partial x$ satisfies the continuity equation (2). In order to simplify the mathematical analysis of the problem, we introduce the following similarity variables

$$\eta = \left(\frac{a}{\upsilon_f}\right)^{\frac{1}{2}} y\,,\ \ \psi = \left(a\upsilon_f\right)^{\frac{1}{2}} x f(\eta)\,,\ \ \theta(\eta) = \frac{T - T_\infty}{T_f - T_\infty}. \tag{7}$$

Using equation (7), equations (3) – (6) are transformed to a set of couple nonlinear ordinary differential equations

$$\left(1 + \frac{1}{\beta}\right)\frac{d^2 f}{d\eta^2} + f\frac{d^2 f}{d\eta^2} + \left(\frac{df}{d\eta}\right)^2 + Gr\theta - M\left(\frac{df}{d\eta} - 1\right) + 1 = 0, \tag{8}$$

$$\frac{d^2\theta}{d\eta^2} + Prf\frac{d\theta}{d\eta} + \left(1 + \frac{1}{\beta}\right)PrEc\left(\frac{d^2 f}{d\eta^2}\right) + PrEcM\left(\frac{df}{d\eta} - 1\right)^2 = 0, \tag{9}$$

with dimensionless boundary conditions

$$f(0) = 0,\ \ \frac{df}{d\eta}(0) = \lambda,\ \ \frac{d\theta}{d\eta}(0) = Bi[\theta(0) - 1],\ \ \frac{df}{d\eta}(\infty) = 1,\ \ \frac{d\theta}{d\eta}(\infty) = 0. \tag{10}$$

From equations (8), (9) and (10), prime denotes differentiation with respect to η, λ is the velocity ratio parameter, Gr is Grashof number, M is magnetic field parameter, Pr is Prandtl number, Ec is Eckert number and Bi is the Biot number respectively defined as follows:

$$\lambda = \frac{b}{a};\ \ Gr = \frac{g\beta(T_w - T_\infty)}{U_\infty a};\ \ M = \frac{\sigma B_0^2}{\rho a};\ \ Pr = \frac{\upsilon}{\alpha};\ \ Ec = \frac{U_\infty^2}{c_p(T_w - T_\infty)};\ \ Bi = \frac{h}{k}\sqrt{\frac{\upsilon}{a}}. \tag{11}$$

The physical quantities of practical interest are the skin friction coefficient C_f and local Nusselt number Nu_x defined as

$$C_f = \frac{\tau_w}{\rho U_w^2}\ ;\ \ Nu_x = \frac{xq_w}{\alpha(T_w - T_\infty)} \tag{12}$$

where, τ_w is the shear stress or skin friction along the stretching sheet and q_w is the heat flux from the sheet and defined as

$$C_f(Re_x)^{\frac{1}{2}} = \left(1 + \frac{1}{\beta}\right)\frac{d^2 f}{d\eta^2}(0);\ \ \frac{Nu_x}{(Re_x)^{\frac{1}{2}}} = -\frac{d\theta}{d\eta}(0) \tag{13}$$

where $Re_x = U_w x/\upsilon$ is the local Reynolds number.

NUMERICAL SOLUTION

The set of couple nonlinear ordinary differential equations (8) and (9) with boundary conditions equation (10) are computed numerically using the shooting method with Runge-Kutta Fehlberg integration scheme. This method involves transforming the dimensionless coupled nonlinear differential equations into a set of first order differential equations after which, the fourth order Runge-Kutta Fehlberg integration scheme is employed until the given boundary conditions are satisfied.

Thus, we define the new variables as;

$$x_1 = f,\qquad x_2 = f',\qquad x_3 = f'',\qquad x_4 = \theta,\qquad x_5 = \theta' \tag{14}$$

Equations (8) – (10) are then reduced to the following system

$$x_2' = \left(\frac{1}{1+\beta}\right)\left(-x_1x_3 - (x_2)^2 - Grx_4 + M(x_2 - 1) - 1\right) \tag{15}$$

$$x_5' = -Prx_1x_5 - \left(1 + \frac{1}{\beta}\right)PrEc(x_3)^2 - MPrEc(x_2 - 1)^2 \tag{16}$$

subject to the following initial conditions,

$$x_1(0) = 0,\ \ x_2(0) = \lambda,\ \ x_5(0) = Bi[\theta(0) - 1],\ \ x_2(0) = s_1,\ \ x_5(0) = s_2 \tag{17}$$

Using the unknown initial conditions s_1 and s_2 in equation (17), equations (15) and (16) are integrated numerically. The accuracy of the assumed missing initial conditions is checked by comparing the calculated value of the dependent variable at the terminal point with its given value there. The accuracy and robustness for solving the boundary value problems confirms with Mutuku (2016). From the process of numerical computation, the fluid velocity $f'(\eta)$ and temperature $\theta(\eta)$ are compared with the given boundary conditions.

RESULTS AND DISCUSSION

The numerical computations are carried out for the various values of the physical parameter with Runge-Kutta Fehlberg integration scheme. The effects of the varying physical parameters: magnetic field parameter (M), Casson parameter (β), velocity ratio parameter (λ), Grashof number (Gr), Biot number (Bi), Eckert number (Ec) and Prandtl number (Pr) on velocity and temperature profiles has been analyzed. The obtained computation results are presented graphically in Fig. 1 – Fig. 8 and discussed.

The effects of various values of magnetic field parameter M on the flow field velocity and temperature profiles are displayed in Figs. 1 and 2. As M increases, the flow field velocity decreases and also increases with decreasing values in M. Due to the Lorentz force induced by the dual actions of electric and magnetic fields, the velocity boundary layer thickness decreases. Similarly, for $\lambda = 0.2$, the temperature profiles increases with increasing values of M. The obtained result is in agreement with Bhattacharyya (2013) and Medikare *et al*., (2016).

Fig. 3 and Fig. 4 present the effects of Casson parameter (β) on the velocity and temperature fields. It is observed from Fig. 3 that the fluid velocity profiles decreases as β increases. Thus, due to the increase in β, the yield stress P_y reduces and consequently, the velocity boundary layer thickness reduces. Fig. 4 shows the influences of Casson parameters on the temperature profiles. It shows that temperature decreases with increasing values in β. This implies that thermal boundary layer decreases (Medikare *et al*., 2016). Fig. 5 presents the effects of temperature profiles for varying values of Biot number Bi. It depicts that increasing values of Bi, decreases in temperature profiles. However, as the flow field moves far away from the sheet within the thermal boundary layer, Biot number varnishes.

The velocity profile for various values of velocity ratio parameter λ is shown in Fig. 6. As described by Mastapha and Gupta (2001) and Bhattacharyya (2013b) for Newtonian fluid, the velocity of fluid inside the boundary layer decreases from the surface towards the edge of the layer for the first kind $(\lambda < 1)$ and the fluid velocity increases from the surface towards the edge for the second kind $(\lambda > 1)$. Similarly, it is important to note that the stretching velocity and straining velocity are equal as such there is no boundary layer of Casson fluid flow near the sheet (Chaim, 1994). The velocity profiles for different values of Grashof number Gr is displayed in Fig. 7. It revealed that the flow field velocity decreases with increasing values of Grashof number Gr thereby reducing the thermal boundary layer along the sheet. The viscous dissipation effect on temperature profiles is shown in Fig. 8. It illustrates that temperature increases with increase in Eckert number (viscous dissipation parameter). The Eckert number Ec produces heat due to drag between the fluid particles causing an increase of the initial fluid temperature due to the extra heat. However, Ec may not only cause thermal reversal but also increases the thermal boundary layer (Medikare et al., 2016).

Fig. 9 shows the effects of Prandtl number Pr of temperature profiles. It depicts that temperature initially increases with increasing values of Prandtl number Pr and later decreases with increased values of Pr towards the thermal boundary layer. The use of Prandtl number in heat transfer problems reduces the relative thickening of the momentum and the thermal boundary layer (Medikare *et al*., 2016). Thus, the rate of heat transfer is enhanced with Pr causing the reduction of the thermal boundary layer thickness.

CONCLUSION

The magnetohydrodynamic SPF of a Casson fluid towards a convectively heated stretching/shrinking sheet is investigated taking the buoyancy force into account. Using the similarity variables, the governing differential equations are transformed to ordinary differential equations and solved numerically by shooting method with Runge-Kutta Fehlberg integration scheme. The effects of the various governing physical parameters were analysed and the following conclusions are drawn:

a. The velocity boundary layer thickness reduces with increasing values of the magnetic field parameter.
b. The flow field velocity decreases with increase in Casson parameter β as well as the thermal boundary layer thickness.
c. The Biot number Bi, decreases the thermal boundary layer thickness whereas the Eckert number Ec increases away from the sheet towards the thermal boundary layer.

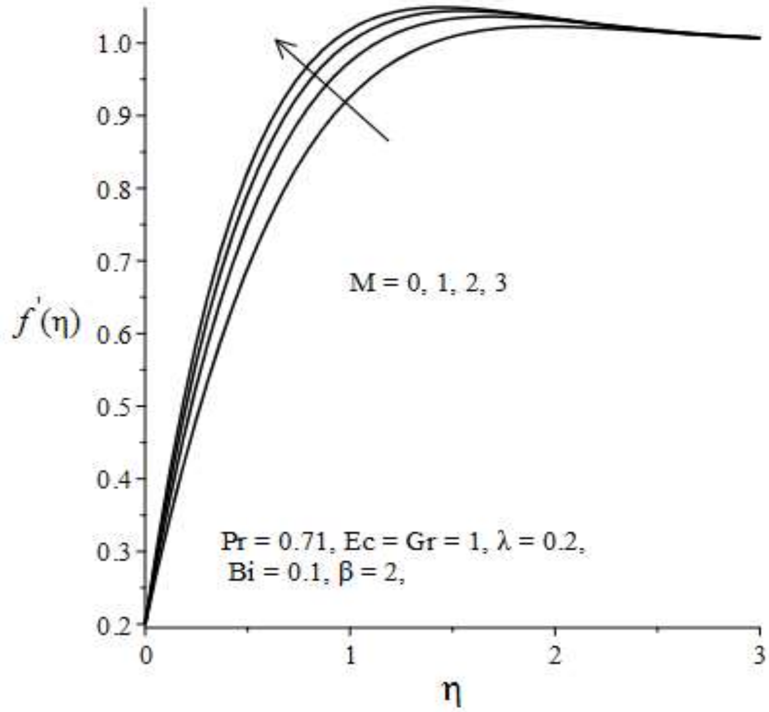

Fig. 1 Velocity profiles for different values of M.

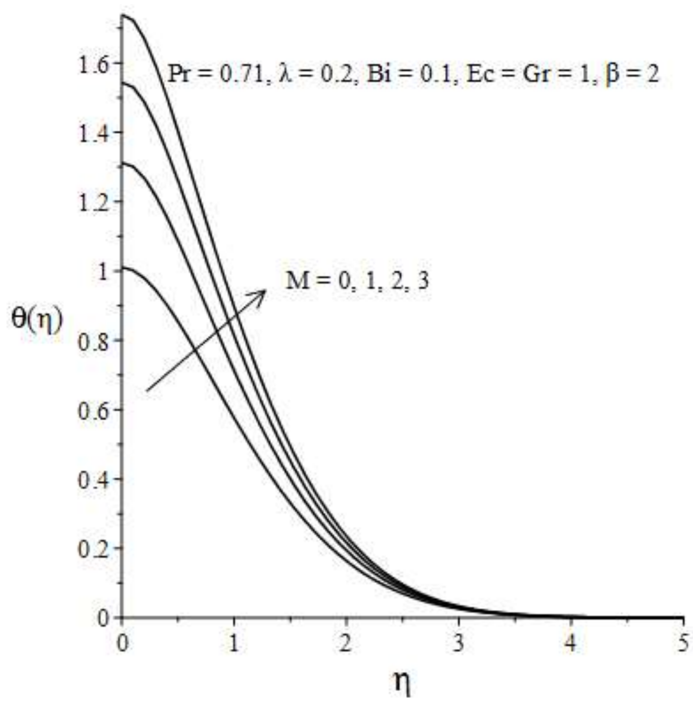

Fig. 2 Temperature profiles for different values of M.

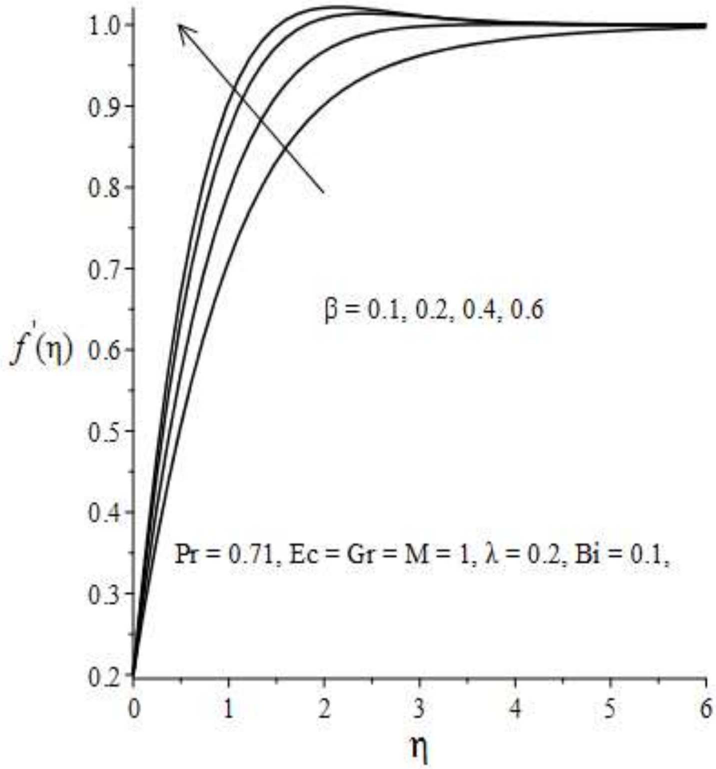

Fig. 3 Velocity profiles for various values of Casson parameter β

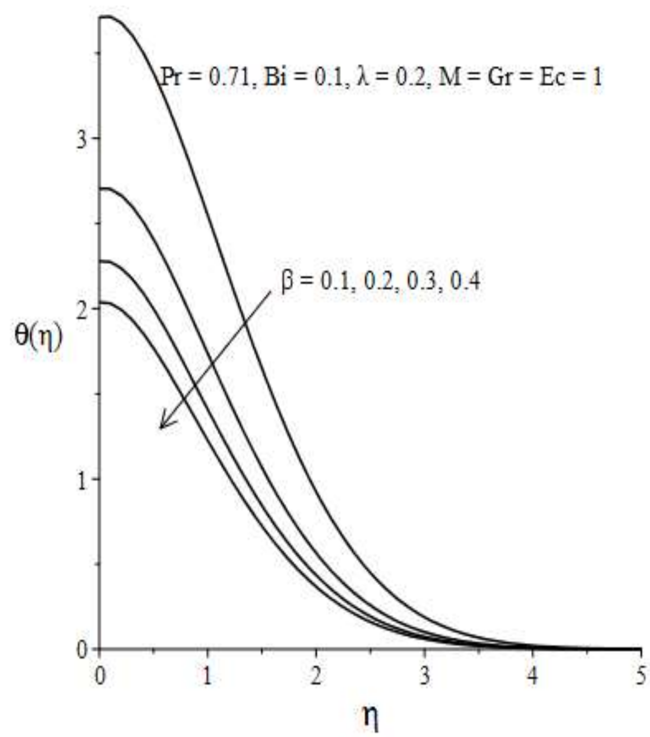

Fig. 4 Temperature profiles for different values of β

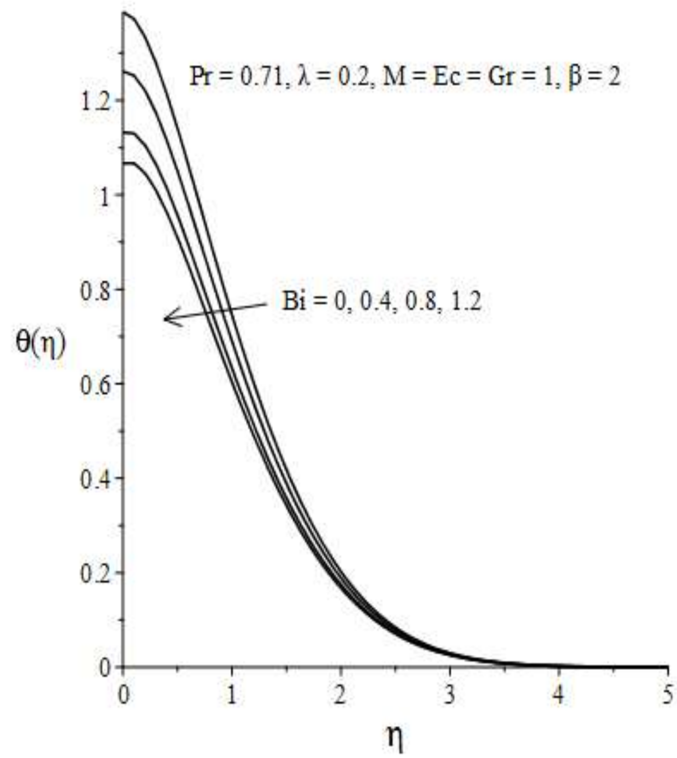

Fig. 5 Temperature profiles for different values of Biot number Bi

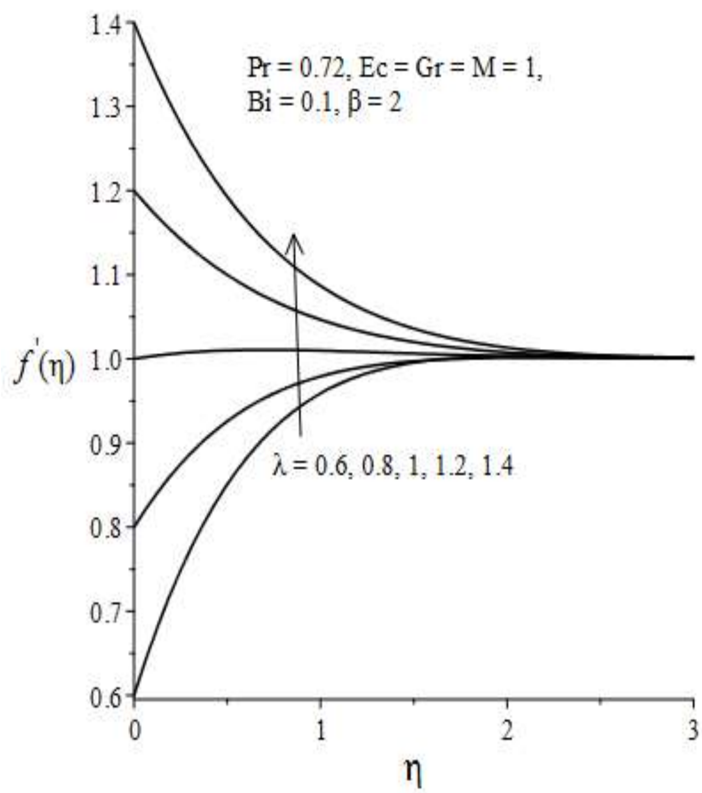

Fig. 6 Velocity profiles for varying values of λ

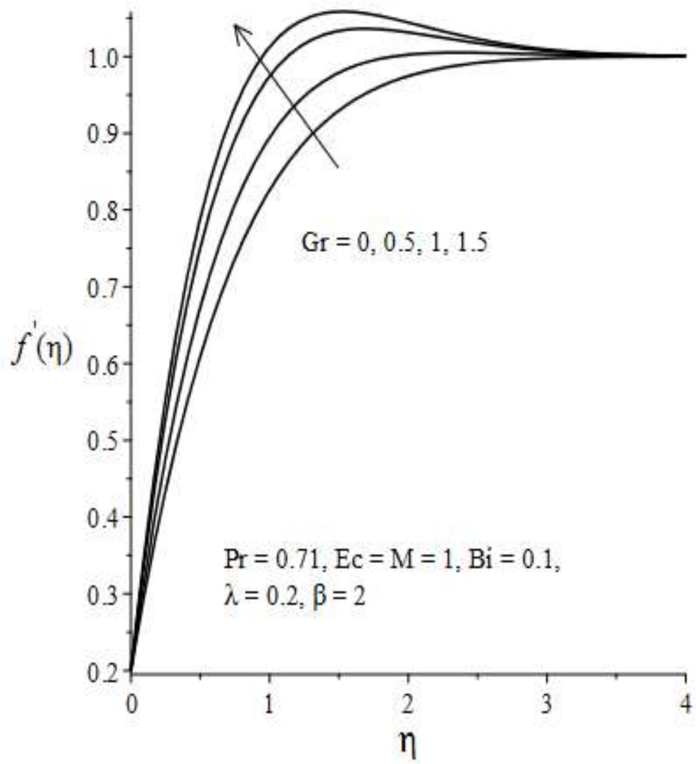

Fig. 7 Effects of various values of Gr on velocity profiles

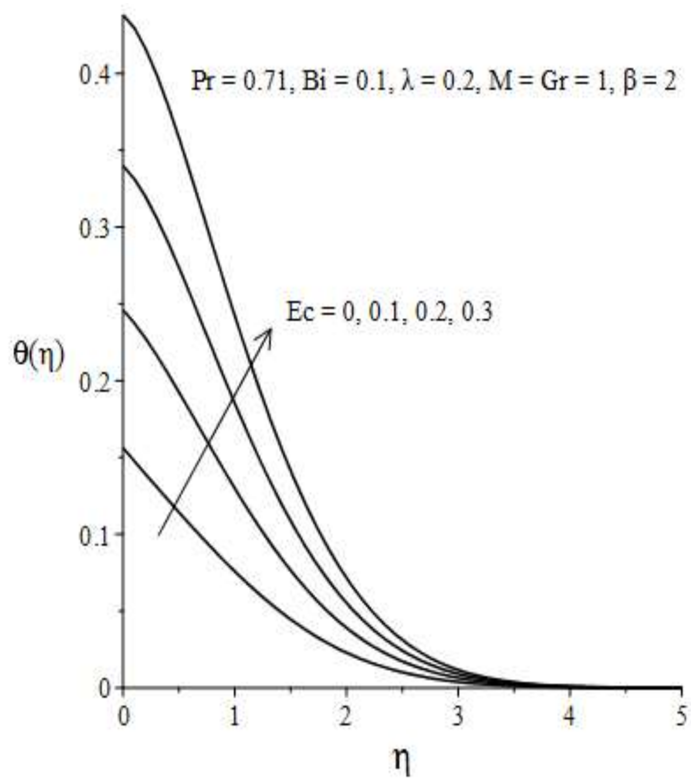

Fig. 8 Temperature profiles for various values of Ec

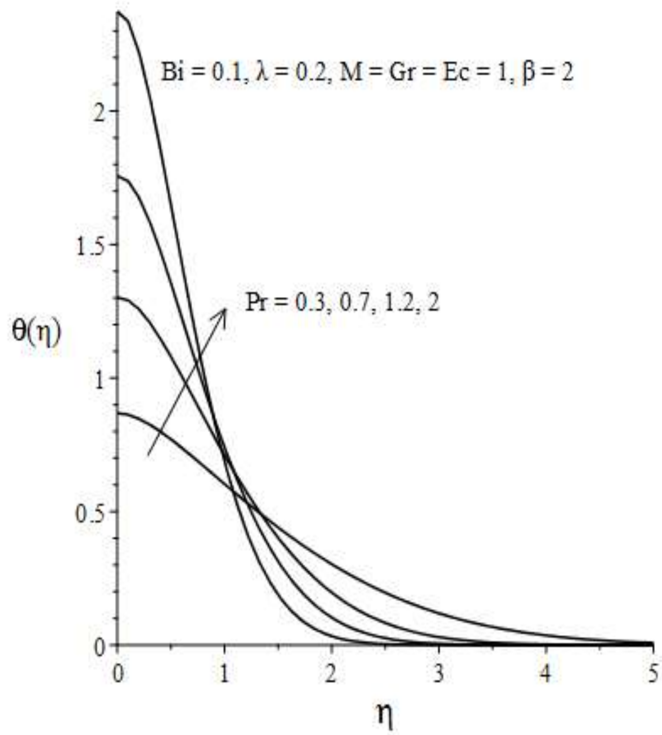

Fig. 9 Effects of different values of Pr on temperature profiles

ACKNOWLEDGMENT

The Authors wish to acknowledge all reviewers of the manuscript for their time in evaluating the content towards a better output.

REFERENCES

Sakiadis, B. C. (1961). Boundary-layer behaviour of continuous solid surfaces: I. boundary-layer equations for two-dimensional and axisymmetric flow. *AIChE Journal, 7(1): 26–28*. https://doi.org/10.1002/aic.690070108

Makinde, O. D. and Aziz, A. (2010). MHD mixed convection from a vertical plate embedded in a porous medium with a convective boundary condition. *Int. J. of Therm. Sci., 49(9): 1813-1820*. https://doi.org/10.1016/j.ijthermalsci.2010.05.015

Bachok, N., Ishak, A. and Pop, I. (2012). Boundary layer flow over a moving surface in a nanofluid with suction or injection. *Acta Mech. Sin., 28(1): 34-40.*

Mutuku, W. N. and Makinde, O. D. (2014). On hydromagnetic boundary layer flow of nanofluids over a permeable moving surface with newtonian heating. *Latin American Applied Research, 44(1): 57-62*. ISSN 1851-8796

Khan, M. and Khan, W. A. (2016). MHD boundary layer flow of a power-law nanofluid with new mass flux condition. *AIP Advances, 6, 025211*. https://doi.org/10.1063/1.4942201

Makinde, O. D. (2012). Computational modeling of mhd unsteady flow and heat transfer toward a flat plate with navier slip and newtonian heating. *Braz. J. Chem. Eng., 29(2) 159-166*.

Crane, L. J. (1970). Flow past a stretching plate. Zeitschrift für Angewandte Mathematik und Physik, *21: 645-647*. http://dx.doi.org/10.1007/BF01587695

Chen, C. K. and Char, M. I. (1988). Heat transfer of a continuous stretching surface with suction or blowing. *J. Math. Anal. Appl., 135: 568–80*.

Chiam, T. C. 1994 "Stagnation-point flow towards a stretching plate. *J. Phys. Soc. Japan, 63: 2443–4*. http://dx.doi.org/10.1143/JPSJ.63.2443

Layek, G. C., Mukhopadhyay, S. and Samad, S. K. A. (2007). Heat and mass transfer analysis for boundary layer stagnation-point flow towards a heated porous stretching sheet with heat absorption/generation and suction/blowing. *Int. Commun. Heat Mass Transfer, 34: 347–56*.

Makinde, O. D. and Aziz, A. (2011). Boundary layer flow of a nanofluid past a stretching sheet with a convective boundary condition. *Int. J. Therm. Sci., 50: 1326–32*.

Gupta, P. S. and Gupta, A. S. (1977). Heat and mass transfer on a stretching sheet with suction or blowing. *The Canadian Journal of Chemical Engineering, 55: 744-746*. http://dx.doi.org/10.1002/cjce.5450550619

Lun-Shin Yao, Y. and Mamun, M. Md. (2008). Non-Newtonian Fluid Flow on a Flat Plate Part 1: Boundary Layer. *Journal of Thermophysics and Heat Transfer, 22(4): 758-761*. http://dx.doi.org/10.2514/1.35187

Reddy, B. S., Kishan, N. and Rajasekhar, M. N. (2012). MHD boundary layer flow of a non-newtonian power-law fluid on a moving flat plate. *Advances in Applied Science Research, 3(3): 1472-1481*.

Xu, H. and Shi-Jun, L. (2009). Laminar flow and heat transfer in the boundary-layer of non-newtonian fluids over a stretching flat sheet. *Computers and Mathematics with Applications, 57: 1425–1431*.

Fox, V. G., Erickson, L. E. and Fan, L. T. (1969). The laminar boundary layer on a moving continuous flat sheet immersed in a non-newtonian fluid. *AIChE Journal, 15: 327-333*. http://dx.doi.org/10.1002/aic.690150307

Casson, N. (1959). A flow equation for pigment oil suspensions of the printing ink type. In: Mill, C.C., Ed., Rheology of Disperse Systems. Pergamon Press, Oxford, 84-102.

Bhattacharyya, K. (2013a). Boundary layer stagnation-point flow of casson fluid and heat transfer towards a shrinking/sketching sheet. *Frontiers in Heat and Mass Transfer, 4, 023003*. https://doi.org/10.5098/hmt.v4.2.3003

Hussain, T., Shehzad, S. A., Alsaedi, A. Hayat, T. and Ramzan, M. (2015). Flow of casson nanofluid with viscous dissipation and convective conditions: a mathematical model. *Journal of Central South University, 22: 1132-1140*. http://dx.doi.org/10.1007/s11771-015-2625-4

Pramanik, S. (2014). Casson fluid flow and heat transfer past an exponentially porous stretching surface in presence of thermal radiation. *Ain Shams Engineering Journal, 5: 205–212*.

Mustafa, M., Hayat, T., Pop, I. and Aziz, A. (2011). Unsteady boundary layer flow of a casson fluid due to an impulsively started moving flat plate. *Heat Transfer, 40: 563-576*. http://dx.doi.org/10.1002/htj.20358

Medikare, M., Joga, S. and Chidem, K. K. (2016). MHD stagnation point flow of a casson fluid over a nonlinearly stretching sheet with viscous dissipation. *American J. of Comp. Mathematics, 6: 37-48*. http://dx.doi.org/10/4236/ajcm.2016.61005

Mutuku, W. N. (2016). Ethylene glycol (EG) based nanofluids as a coolant for automotive radiator. *Asia Pacific Journal for Computational Engineering, 3(1): 1-15*. https://doi.org/10.1186/s40540-016-0017-3

Mabood, F., Ibrahim, S. M., Kumar, P. V. and W. A. Khan, (2017). Viscous dissipation effects on unsteady mixed convective stagnation point flow using Tiwari-Das nanofluid model. *Results in Physics, 7: 280-287*. http://dx.doi.org/10.1016/j.rinp.2016.12.037

Seth, G. S., Tripathi, R. and Mishra, M. K. (2017). Hydromagnetic thin film flow of casson fluid in non-darcy porous medium with joule dissipation and navier's partial slip. Applied Mathematics and Mechanics, 38: 1613-1626. https://doi.org/10.1007/s10483-017-2272-7

Bhattacharyya, K. (2013b). MHD stagnation-point flow of casson fluid and heat transfer over a stretching sheet with thermal radiation. *Journal of Thermodynamics*. http://dx.doi.org/10.1155.2013/169674

Battacharyya, K. (2011). Dual solution in boundary layer stagnation-point flow and mass transfer with chemical reaction past a stretching/shrinking sheet. *International Communications in Heat and Mass Transfer, 38(7): 917-922*.

Mahapatra, T. R. and Gupta, A. S. (2001). Magnetohydrodynamic stagnation-point flow towards a stretching sheet. *Acta Mechanica, 152(1-4): 191-196*.

Mutuku, W. N. and Makinde, O. D. (2017). Double stratification effects on heat and mass transfer in unsteady mhd nanofluid flow over a flat surface. *Asia Pac. J. Comput. Engin., 4(2)*. https://doi.org/10.1186/s40540-017-0021-2

Saidulu, N. and Lakshmi, A. V. (2016). MHD flow of casson fluid with slip effects over an exponentially porous stretching sheet in presence of thermal radiation, viscous dissipation and heat source/sink. *American Res. J. of Mathematics, 2: 1-15*. ISSN (online) 2378-704X

Ouru, J. O., Mutuku, W. N. and Oke, A. S. (2020). Buoyancy-induced mhd stagnation point flow of williamson fluid with thermal radiation. *Journal of Engineering Research and Reports, 11(4): 9-18*. https://doi.org/10.9734/jerr/2020/v11i417065

El-Aziz, M. A. and Yahya, A. S. (2017). Perturbation analysis of unsteady boundary layer slip flow and heat transfer of casson fluid past a vertical permeable plate with hall current. *Applied Mathematics and Computation, 307: 146-164*. https://doi.org/10.1016/j.amc.2017.02.034

Mutuku, W. N. and Makinde, O. D. (2013). Combined effect of buoyancy force and navier slip on mhd flow of a nanofluid over a convectively heated vertical porous plate. *The Scientific World Journal, 2013*. https://doi.org/10.1155/2013/725643

Mutuku, W. N. (2014). Analysis of hydromagnetic boundary layer flow and heat transfer of nanofluids, Doctoral Thesis, Cape Peninsula University of Technology, South Africa.

Shehzad, S. A., Hayat, T., Qasim, M. and Asghar, S. (2013). Effects of mass transfer on mhd flow of casson fluid with chemical reaction and suction. *Brazillian Journal of Chemical Engineering, 30(1)*. https://doi.org/10.1590/S0104-66322013000100020

Sobamowo, G., Jayesimi, L., Oke, D., Yinusa, A. and Adedibu, O. (2019). Unsteady casson nanofluid squeezing flow between two parallel plates embedded in a porous medium under the influence of magnetic field. *Open Journal of Mathematical Sciences, 3: 59-73*. https://dx.doi.org/10.30538/oms2019.0049

Ferdom, M., Khaleque, T. S. and Bangalee, M. Z. I. "Heat generation and radiation effects on mhd casson fluid flow over stretching surface through porous medium. European J. of Advances in Engineering and technology, 4(11): 859-857.

Sheikh, M. and Abbas, Z. (2017). Homogeneous-heterogeneous reactions in stagnation point flow of casson fluid due to a stretching/shrinking sheet with uniform suction and slip effects. *Ain Shams Engineering Journal, 8(3): 467-474*. https://doi.org/10.1016/j.asej.2015.09.10fcombined

Medikare, M., Joga, S. and Chidem, K. K. (2016). MHD stagnation point flow of a casson fluid over a nonlinearly stretching with viscous dissipation. *American Journal of Computational Mathematics, 6(1): 37-48.* https://dx.doi.org/10.4236/ajcm.ajcm.2016.610005

Singh, M K., Kushvah, B. S., Seth, G. S. and Prakash, J. (2018). Applications of fluid dynamics. In Proceedings of ICAFD 2016 Springer Science and Business Media LLC.

Nandy, S. K. (2013). Analytical solution of mhd stagnation-point flow and heat transfer of casson fluid over a stretching sheet with partial slip. *International Scholarly Research Notices, 2013*. https://doi.org/10.1155/2013/108264

Bhattacharyya, K., Hayat, T. and Alsaedi, A. (2013). Exact solution for boundary layer flow of casson fluid over a permeable stretching/shrinking sheet. *Journal of Applied Mathematics and Mechanics, 94(6)*. https://doi.org/10.1002/zamm.201200031

Mukhopadhyay, S., Mondal, I. C. and Chamka, A. J. (2013). Casson fluid flow and heat transfer past a symmetric wedge. *Heat Transfer, 42(8)*. https://doi.org/10.1002/htj.21065

Gangadhar, K., Kannan, T., Jayalakshmi P. and Sakthivel, G. (2018). Dual solutions for mhd casson fluid over a shrinking sheet with newtonian heating. *International Journal of Ambient Energy, 2018*. https://doi.org/10.1080/01430750.2018.1550018

Shateyi, S. and Marewo, G. T. (2014). Numerical analysis of mhd stagnation-point flow of casson fluid, heat and mass transfer over a stretching sheet. Advances in Applied and Pure Mathematics, 128-132.

Bhattacharyya, K. and Vajravelu, K. (2012). Stagnation-point flow and heat transfer over an exponentially shrinking sheet. *Communications in Nonlinear Science and Numerical Simulation, 17(7): 2728-2734*. https://doi.org/10.1016/j.cnsns.2011.11.011.